A forward model for beam emission spectroscopy at ASDEX Upgrade

R. Dux, B. Geiger, R. M. McDermott, E. Viezzer and the ASDEX Upgrade team
Max-Planck-Institut für Plasmaphysik, Garching, Germany

The ASDEX Upgrade tokamak is equipped with a new charge exchange recombination spectroscopy (CXRS) system, which observes the neutral beam #8 on a dense grid of radially distributed lines-of-sight. The lines-of-sight have a toroidal orientation and measurements are made across the plasma centre up to the high field side. A dedicated spectrometer has been installed to monitor the D_α emission of the beam atoms, which can deliver an almost direct measure of the neutral beam density [1]. Since the uncertainty of the neutral beam density from beam attenuation calculations increases with the path length of the beam in the plasma, a direct measure is especially important for the measurements on the high field side.

For the above application, a model of the beam emission spectrum has been developed in order to simplify the fit of the complicated spectral feature, where each beam species (full, half and third energy component) contributes with a D_α multiplet consisting of 9 spectral lines. In addition, the spectrum is overlapped by the D_α radiation of the beam halo and a CII multiplet. The model was compared with first measurements.

Beam Emission Spectrum

The standard value for the acceleration voltage of beam 8 is 93 keV for deuterium operation. The atoms with 93 keV energy carry about 63% of the beam power, while the atoms at half and third energy contribute 28% and 9% respectively. At these energies, the line splitting of the D_α spectrum in the magnetic field of the tokamak is determined by the Stark effect due to the electric field $\vec{F} = \vec{v} \times \vec{B}$ in the rest frame of the fast atoms (motional Stark effect, MSE). It produces a symmetric multiplet of 15 lines, where the very weak 6 outermost lines can be neglected. The line splitting is proportional to the electric field F, i.e. the velocity v of the atom, the magnetic field strength B and the angle φ between $\vec{v}$ and $\vec{B}$: $\Delta\lambda_{\mathrm{MSE}}[\mathrm{nm}] = 2.76\times10^{-8}\Delta k F[\mathrm{V/m}]$ with Δk=-4,-3,...,4 and $F = vB\sin\varphi$. The line strength varies with the angle ψ between $\vec{F}$ and the direction $\vec{k}$ of the emitted radiation: for the 3 innermost σ-lines $L_\sigma = L_{\sigma,90}(1+\cos^2\psi)$ and for the remaining π-lines $L_\pi = L_{\pi,90}(1-\cos^2\psi)$. For ψ=90^o and equal population of all upper states, the line ratios $L_{\sigma,0}$:$L_{\sigma,\pm1}$:$L_{\pi,\pm2}$:$L_{\pi,\pm3}$:$L_{\pi,\pm4}$ are 5490:1936:729:2304:1681 [2]. However in tokamak plasmas, deviations from these line ratios have been found [3] and were modelled to be caused by a non-statistical population of the sub-levels of the upper $n = 3$ states [4]. When denoting the upper states with $|nkm\rangle$, i.e. with the electric quantum number k and the magnetic quantum number m for the angular momentum about the direction of $\vec{F}$, the modelling found equal population of states with same values of $|k|$ and $|m|$. Thus, there are three independent occupation numbers $b_{|k|,|m|}$, which describe the non-statistical population, e.g. $b_{0,2}$, $b_{1,1}$ and $b_{2,0}$, while the forth number $b_{0,0}$ follows from the normalisation condition: $n^2 = b_{0,0} + 4b_{1,1} + 2(b_{2,0} + b_{0,2})$. The above line ratios are then (882$b_{0,0}$+4608$b_{0,2}$):1936 $b_{1,1}$:729 $b_{0,0}$:2304 $b_{1,1}$:1681 $b_{2,0}$. For our measurements on the high-field side, the D_α multiplet is very well resolved and first fits (see below) give typical values of $b_{0,0}$=1.05, $b_{0,2}$=0.84, $b_{1,1}$=1.00, and $b_{2,0}$=1.13, which leads to a suppression of the central σ0-line and an increase of the outer π4-lines. In the model function, the spectra of all beam species are calculated with the same b-values, which presently are fit parameters but might be fixed later. For the atoms

at 31 keV, the inclusion of the Paschen-Back effect starts to produce deviations from the above simple ψ-dependence. For the lines-of-sight on the high-field side, the σ-lines are reduced by up to about 5% and the π-lines are increased by up to about 7%. The line shift is still well represented by the pure MSE-formula. Finally, the line shift due to the Doppler effect has to be taken into account which depends on the angle α between $\vec{\mathrm{v}}$ and $\vec{k}$: $\Delta\lambda_{\mathrm{Dop}} = -\lambda_0 \mathrm{v} \cos\alpha / c$.

For the calculation of the spectrum, the velocity distribution $F(\vec{\mathrm{v}}, \vec{x})$ of the beam atoms for all points along the line-of-sight $\vec{x} = \vec{x}_0 + l\vec{k}$ is needed. It is usually calculated with Monte Carlo models. Here, we use the same basic assumptions as in the Monte Carlo models but replace the individual holes (774 for the beams at ASDEX Upgrade) of the extraction grid by a continuously emitting surface, which leads to rather simple analytic expressions. Each point on a grid emits the same number of atoms per second. The mean starting velocity is directed to a horizontal and vertical focus and the velocity direction has an angular spread, which is described by a Gaussian distribution. Thus, the velocity distribution function just depends on the orientation $\vec{u} = \vec{\mathrm{v}}/\mathrm{v}$ of the velocity while the absolute value is fixed. Furthermore, it is the product of two distributions functions in the two directions perpendicular to the beam direction, which we denote here by x and y, i.e. $F(\vec{\mathrm{v}}, \vec{x}) = F(u_x, u_y, \vec{x}) = F_x(u_x, x, z) F_y(u_y, y, z)$. For a certain transition $n \to m$ of the MSE multiplet, the line shape function $S_{n\to m}(\lambda)$ at wavelength λ is given by an integration over the LOS and the velocity orientations.

$$S_{n\to m}(\lambda) = \int_{-\infty}^{\infty} dl \int_{-\infty}^{\infty} du_x \int_{-\infty}^{\infty} du_y F(u_x, u_y, l) w_{n\to m}(u_x, u_y, l) \delta[\lambda - \lambda_{n\to m}(\mathrm{v}, u_x, u_y, l)]$$

Here, $\lambda_{n\to m}(\mathrm{v}, u_x, u_y, l)$ is the wavelength of the D_α line being shifted due to the Doppler effect and the motional Stark effect, $w_{n\to m}(u_x, u_y, l)$ is a weighting function, which takes variations of the beam attenuation, beam excitation, and the emission into direction $\vec{k}$ into account and $\delta[\lambda - \lambda_{n\to m}]$ represents the δ-function.

The above integral for the line shape has to be numerically calculated. Fig.1 illustrates the main elements, which contribute to the integral for 2 lines-of-sight. The sightline 'COR-67' (left column) intersects the beam on the high-field side at a major radius R=1.22 m and 'COR-25' (right column) at the low-field side at R=1.82 m. The upper three boxes of each column show profiles along the sightline coordinate l, where we use the distance Δl to the point with maximum D_α emission. The profile of the D_α emission ε into all directions is displayed in the upper box. It has been calculated with a collisional radiative model yielding the beam attenuation and the beam excitation along the beam. It is wider for the LOS on the high-field side since the beam is intersected at a smaller angle. The product of ε with the ψ-term from above yields the weight w of the integral. However, the variation of this ψ-factor is not so large and the shape of w is dominated by ε. The next lower boxes show the profiles, which determine the line shifts. $\Delta\lambda_{\mathrm{MSE}}$ is proportional to the magnetic field strength B, which is normalised to its value at Δl=0. It does not vary a lot along the intersection region and is about 50% larger on the LOS at the high-field side. All following quantities depend on $\vec{\mathrm{v}}$ and only the corresponding mean values of the velocity distribution at this point are plotted. The $\sin\varphi$-term contributing to $\Delta\lambda_{\mathrm{MSE}}$ shows a considerable variation, especially on the high-field side, where it changes by about a factor of 2. The variation of the $\cos\alpha$-term of the Doppler shift is 27% larger on the low-field side LOS since it is more perpendicular to the beam. The boxes on the next line display the average wavelength difference of three lines

with respect to the wavelength at the emission maximum (Δl=0). The central σ0-line is only affected by the Doppler shift and the part of the LOS, which is closer to the observer (Δl <0), is blue shifted compared to Δl=0, while it is red shifted for Δl >0. For the outermost π-4 line on the blue side of the multiplet, the variation of $\Delta\lambda_{\mathrm{MSE}}$ and $\Delta\lambda_{\mathrm{Dop}}$ across the intersection region add up and the blue/red-shift with respect to the emission at Δl=0 increases, especially, for the LOS on the high-field side. For the outermost π4 line on the red side of the multiplet, the MSE- and Doppler-shift variation have opposite sign. For 'COR-25', the total line shift variation is just somewhat reduced. However, on the high-field side, the MSE-shift is so strong, that the far side of the LOS now contributes to the blue line wing, while at the near side, the average line shift is almost constant with a maximum of $\langle\Delta\lambda\rangle\approx$0 nm. In the lowest boxes, the line shape function S_λ (normalised to area 1) is plotted versus the wavelength difference $\Delta\lambda$ to the average wavelength at the emission maximum. For the low-field side, the shapes are still Gaussian like, while the outermost π-lines on the high-field side develop asymmetrical non-Gaussian shapes.

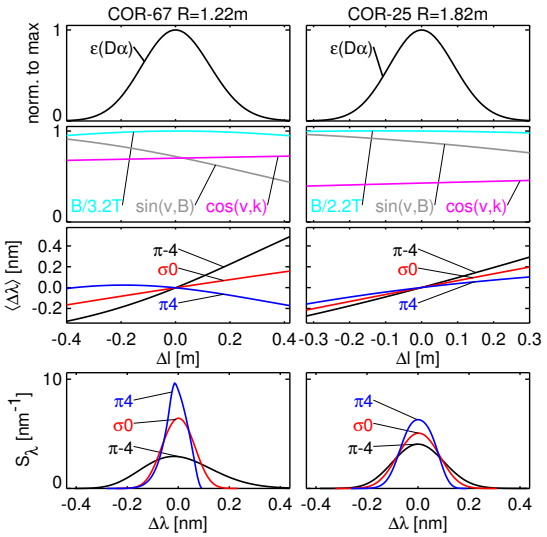

Fig.1: *The spectral shape of some lines from the D_α multiplet (lower boxes) and profiles along the sightline, which lead to these shapes (upper three boxes) for 2 lines-of-sight: left on the high-field side and right on the low-field side.*

For Fig.1, the atom energy was set to 93 keV. The shifts scale linearly with the velocity v and the line shapes of the other beam species are just a factor v more narrow since the weighting function w is very weakly depending on v. Thus, the line shapes are only calculated for one beam energy and rescaled with the corresponding beam velocity during the fit. Furthermore, it turns out, that besides the product $Bsin\varphi$ at Δl=0, all other discharge dependent parameters have only a minor influence on w or the change of $Bsin\varphi$ across the intersection region, such that the line shapes can be calculated before the fit for all LOS and MSE lines on a grid of values of $Bsin\varphi$ at Δl=0 and saved in a lookup table, which is then used to compute the actual line shape by linear interpolation.

The shape of the MSE spectrum is thus fixed and only the line strength due to the three energy components of the beam are free parameters in the fit function. An integral part of the beam emission spectrum is the broad line due to the beam halo, whose radiance is a few times stronger than the MSE features. The halo emission is unpolarised and well described by a shifted Gaussian. At present, we either use T_i and v_{rot} from the CXRS diagnostic to define the line position and shape or leave it together with the radiance of the halo as free parameters in the fit. The CII doublet $2s^2 3p\,{}^2P_{3/2,1/2} \rightarrow 2s^2 3s\,{}^2S_{1/2}$ at 657.8 nm and 658.3 nm is another prominent feature overlapping with the beam emission spectra. We fix the normalised flux surface coordinate of the emission region to ρ_{pol}=1.02, i.e. in the scrape-off layer, and calculate for the two intersections of the LOS and the corresponding flux surface the B field and the angle between $\vec{B}$ and $\vec{k}$. This defines the Zeeman splitting and the relative weight of σ- and π-lines of the Zeeman multiplet. Each multiplet line is given a Gaussian shape corresponding to a low ion temperature

around 10 eV. The spectra of the two intersection points are added up, normalised to an area of 1, and multiplied with the line radiance of the total CII doublet, which is a further fit parameter. Finally, the spectrum is folded with the instrumental line shape and a constant background is the last fit parameter. At present, we neglect the FIDA emission in the model function.

Fig.2 shows two fits of the model to measured spectra on the same LOS as previously used in Fig.1. The spectra are a temporal average from 2-2.1s from #31484, an H-mode plasma with B_T=2.5 T, I_p=0.8 MA, and line averaged density n_e=5.3×10^{19} m^{-3}. The data are taken with a preliminary spectrometer setup, where the spectral region does not extend up to the blue side of the unshifted D$_\alpha$ line, such that the halo is not well seen in the data. The upper spectrum is from the high-field side, where the maximum of the MSE emission is at $\rho_{pol,max}$=0.93 while the lower graph is from the low-field side with $\rho_{pol,max}$=0.32. In this low density discharge, the MSE features can nicely be measured on the high-field side (note, the change of the scale of the spectral radiance!). The data are shown by the grey crosses, while the fit is shown as a black line. The model spectrum of the beam species with full, half and third energy is depicted by a blue, green and red line. The CII-multiplet is given by a cyan line and the halo is shown in magenta. The basic behaviour of the line shapes of the MSE feature is well described by the fit. A close inspection of the line widths yields that the model fits the measured widths only within ±10%, i.e. too wide for the σ0-line, but too narrow for the π-lines on the red side of the spectrum for the high-field side LOS and again too wide for the same lines at the low-field side LOS. Given the restricted knowledge about the velocity distribution function of the beam and the simplifying beam model, this fit is still considered to describe the spectra reasonably well. When applying the fit to all LOS, the line radiance of D$_\alpha$ of all beam species can be well fitted up to the innermost LOS on the HFS and will be used to study LFS/HFS impurity density asymmetries based on an experimentally verified beam attenuation.

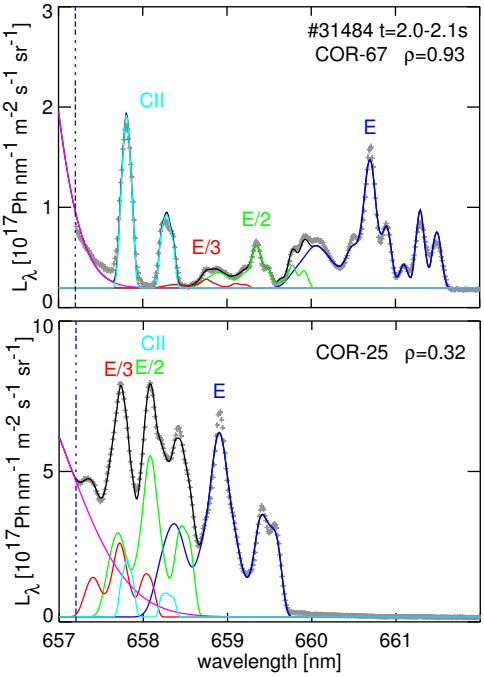

Fig.2: *Measured an fitted spectral radiances for the same LOS as in Fig.1.*

Acknowledgement

This work has been carried out within the framework of the EUROfusion Consortium and has received funding from the Euratom research and training programme 2014-2018 under grant agreement No 633053. The views and opinions expressed herein do not necessarily reflect those of the European Commission.

References

[1] B. Geiger et al, this proceeding (2015) P1.116.
[2] E. Schrödinger et al, Ann. d. Phys. **80**(1926)468.
[3] E. Delabie et al, Plasm. Phys. Control. Fusion **52**(2010)125008.
[4] O. Marchuk et al, J. Phys. B: At. Mol. Opt. Phys. **43** (2010) 011002.